



Resolving the Volumetric Flow Field Inside a Cylindrical Water Ladle Model with Gas Stirring

Yasmeen Jojo-Cunningham, Xipeng Guo, Chenn Zhou, and Yun Liu^(✉)

Purdue University Northwest, Hammond, IN 46323, USA

liu739@pnw.edu

Abstract. Although ladle metallurgy plays a critical role in steelmaking by stirring the molten steel to gain active control over the steel's composition and properties, the physical processes of molten steel flow inside a ladle lack clarity due to its inherent difficulties of perceiving under the extreme conditions. Thus, improving our understanding of the flow processes, particularly inclusion formation and removal mechanisms in steel refining through the stirred flow field, would allow potential enhancement in steelmaking's efficiency and quality. In this project, an advanced Particle-Tracking-Velocimetry system of Shake-the-Box was implemented on a cylindrical water ladle model, made of plexi-glass with compressed air injections through two circular plugs at the bottom, to resolve the three-dimensional flow field inside a $6 \times 6 \times 2$ cm domain. To suppress the flow image distortion due to the curved plexi-glass wall, the method of refractive matching was utilized with an outer polygon tank and sodium iodide solution. Totally, eight conditions of compressed air injection were investigated revealing a highly unsteady and three-dimensional flow field inside the water ladle model.

Keywords: Ladle Metallurgy · Water Ladle model · Volumetric Flow Field · Shake-the-Box system

1 Introduction

In the secondary steelmaking process, the refining of the molten metal from the primary process, gas stirring is a critical operation that involves injecting an inert gas into the molten metal to achieve uniform mixing. It facilitates the homogenization of the chemical composition of alloy elements and the removal of inclusions from the molten steel. The use of stirring aids enhances the quality and purity of the steel, improves its mechanical properties, and minimizes defects in the final product. Furthermore, gas stirring increases the efficiency of alloying and deoxidation, which leads to substantial cost saving and process improvements. The injection of inert gas from the bottom of the ladle into the molten steel creates a slag eye, which is a depression in the slag layer caused by gas bubbles rising from the bottom of the ladle. The behavior of the slag layer is a critical factor in the liquid metal refinement process, as the interaction between the liquid metal and the slag is more prominent in the region surrounding the slag eye compared to

other areas in the ladle. The formation of the slag eye facilitates the efficient removal of impurities and inclusions in the molten steel, leading to an enhancement in overall quality and purity. Over the past few decades, researchers have extensively studied the formation of slag eye in a gas stirred ladles. To study this phenomenon, in a practical application, an equivalent scaled simplified water model apparatus has been used, which involves using water at room temperature instead of molten steel. Water at room temperature has the similar kinetic viscosity to molten steel [1], and thus the properly scaled water ladle apparatus is a suitable substitution of steel ladles to be studied for understanding the related flow process.

The use of physical modeling in studying the flow characteristics of molten steel during the secondary steelmaking process has been a topic of interest for researchers for several decades. Szekely et al. [2] first created a simplified water model to study the flow characteristics of a ladle by injecting gas from the bottom, assuming a constant bubble size, and using Spalding's $k-\omega$ model to solve the Navier-Stokes equations for velocity and turbulence predictions. The model was developed to simulate the thermal and flow behavior of molten steel during the pouring process using a water-cooled ladle by offering a simple and effective way to predict the behavior of molten steel during pouring by its simple geometry of the ladle and assuming that the thermal and flow behavior could be accurately represented by a single stream of fluid flowing from the ladle spout. Debroy et al. [3] improved Szekely's model by refining the bubble model and accounting for the effects of turbulence and bubble coalescence. These added terms helped to predict the behavior of bubbles more accurately in the liquid metal and their impact on the mixing and refining of the steel. Johansen et al. [4] furthered the research by discovering that bubbles can create turbulence and affect flow velocity in the bubble plume region thus adapting a bottom injection water model. Peranandhantan et al. [5] conducted an experiment to study the behavior of the slag eye in a ladle during steelmaking process by injecting air into a ladle filled with water to simulate the injection of gas into molten steel. The researchers then measured the size and shape of the slag eye using high-speed photography and image analysis techniques. Based on their observation from multiple variables tested including gas flow rate, slag thickness, liquid depth, an empirical expression was developed to formulate the slag eye size in terms of the gas flow rate, the dimensions of the ladle, gravity, surface tension, and the momentum of the gas bubbles on the behavior of the slag eye. Mazumdar et al. [6] reviewed several studies related to the physical modeling and empirical correlation of gas-stirred ladles and highlighted the impact of various variables involved in the gas-stirring process, specifically the impact of plug positions. Several researchers experimented with changing the plug positions in their water ladle model to improve better mixing and wall shear stress distribution [6–8]. It is argued that plug design can change the bubble size distribution close to the plug, but not the average size and distribution in the whole ladle [5, 10–12]. In 2019, Owusu et al. [13] used Particle Image Velocimetry (PIV) to investigate the behaviour of bubbles and their effect on turbulence kinetic energy in the cross-sectional plane of the water ladle. So far, many researchers have used PIV method to study the flow field in the ladle, but the study only resolved the flow field results in two-dimensions. The measurement of velocity and turbulence distribution in three-dimension space is still undeveloped. To further investigate the three-dimensional internal flow field in a water ladle model of a

cylindrical container, this study implements a Particle Tracking Velocimetry system with refractive index matching to quantify the unsteady/three-dimensional flow field while minimizing the imaging distortion. Such study cannot only improve our understanding of the complex flow behavior in gas-stirred ladles but also be used to validate the CFD simulation models.

2 Experimental Setup

To achieve the volumetric flow measurement on a cylindrical gas stirred water ladle model, a Particle Tracking Velocimetry system is utilized along with a Refractive Index Matching method. The flow measurements were conducted under eight conditions of gas stirring/injection with a volumetric flow rate ranging from 0.1 LPM to 0.4 LPM. Table 1 summarized the testing conditions of the experiments.

Table 1. Eight test conditions of gas injection flow rate in liters per minute.

| Condition | 1 | 2 | 3 | 4 | 5 | 6 | 7 | 8 |
|--------------|-----|-----|-----|-----|-----|-----|-----|-----|
| Plug 1 [LPM] | 0.1 | 0.2 | 0.3 | 0.4 | 0.1 | 0.2 | 0.3 | 0.4 |
| Plug 2 [LPM] | 0.1 | 0.2 | 0.3 | 0.4 | 0 | 0 | 0 | 0 |

Cylindrical Water Ladle Model and Refractive Index Matching. In this experiment, a cylindrical container with an inner diameter of 2.75 in (70 mm) is implemented to simulate the cylindrical ladle. Due to the curved surface of the cylindrical container that would introduce significant particle image distortion from refraction, the conventional flow field measurement methods, such as Particle Image Velocimetry and Particle Tracking Velocimetry, cannot be directly implemented to measure the flow field. Therefore, this study adopted the refractive index matching method to eliminate image distortion from refraction. Additionally, to film the particle images from four different perspectives, a four-camera particle tracking velocimetry system was utilized on a larger hexagon tank with six flat walls built accordingly to accommodate the angle of imaging. This larger hexagon tank was designed to allow the cameras to film the flow inside the cylindrical tank, which was positioned at the center of the larger hexagon tank, with the cameras filming perpendicular to the flat walls. Both tanks were made of plexi-glasses, and a Sodium Iodide solution was prepared and used to fill the tanks to a solution height of 3 in. As the solution has a refractive index close to plexi-glass, the scattered light from the seeding particles can pass through the curved plexi-glass wall and solution with minimum light refraction, eliminating particle image distortion when the Particle Tracking Velocimetry is employed.

Particle Tracking Velocimetry System. The state-of-the-art: Shake-the-Box system (Lavisson, Gottingen) is implemented on the cylindrical water ladle model, which inject compressed air to stir the flow. Hollow glass spheres (diameter of 8–12 μm) are used as seeding particles in the ladle model to track the gas stirred water flow. To capture the

seeding particles in the flow field and film the particle images, a high repetition rate laser (Nd: YLF single cavity, Photonics DM-30-527) and four high-speed cameras (Phantom VEO 640), mounted on two sides, were utilized. The imaging system included lenses (Tokina Macro) with a focal length of 100 mms and aperture size of $f - 4.5$. Cylindrical optical lenses are added to the laser head to generate a 20 mm thick laser light that penetrates and illuminates the inner cylindrical tank from the side. To measure the flow field from the injection plugs, the sampling frequency of the images/laser was set at 100 Hz with an image resolution of 1024×1024 pixels on all the four high-speed cameras, resolving the three-dimensional flow field within a volume of $6 \times 6 \times 2$ cm domain. Calibration, data collection and velocity field constructions are realized using the software Davis 10 (LaVision, Gottingen). A 55×55 mm calibrate target was utilized and placed in the field of view in the Sodium Iodide solution to capture images for calibration. Calibration was then performed in the Davis 10 using four images of the target. To improve sub-pixel accuracy and realize the volumetric measurement with the system, volume self-calibration was required by the Shake-the-Box system, which was conducted using particle images taken during the experiments. The Shake-the-Box algorithm (LaVision, Gottingen) was then used to carry out particle reconstruction/tracking by shaking the particle position by 1 voxel during the iterations. The instantaneous volumetric velocity field was eventually reconstructed through the post-processing in the Davis 10, resulting in three $15 \times 13 \times 5$ matrices for the volumetric velocity in the three dimensions with a spatial resolution of 4.7 mm/velocity vector. For details about the algorithm of Shake-The-Box, please refer to Schanz et al. [14].

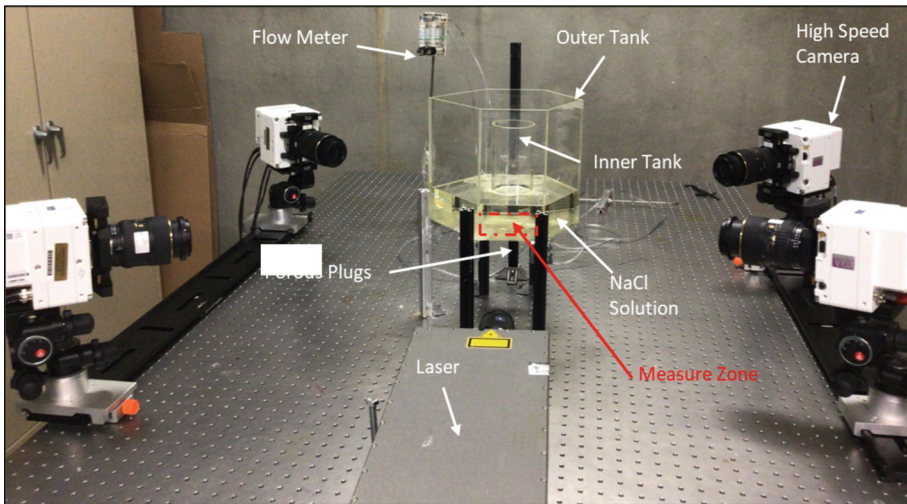


Fig. 1. The Experimental Setup of the Shake-The-Box system

3 Experimental Results

During the experiments, under each testing condition (see Table 1), a total of 2000 data samples (2000 images on each high-speed camera) were taken over a time duration of 20 s, then the seeding particles velocity and trajectories under the 2000-time instants were acquired from the particle tracking process in the Davis 10 software and only the mean velocity field and its characteristics are considered and investigated in this paper.

3.1 Mean Velocity Magnitude

Figure 2 depicts the mean volumetric velocity magnitude field, which exhibits several interesting characteristics of the flow. Specifically, in the case of double gas injection, as the flow rate increasing, the high-velocity region becomes more pronounced, and its location extends from the top towards the bottom of the ladle model. And the high-velocity region is concentrated on the outer edges, specifically on the right-hand side of the ladle model (at the side of $X = 30$ mm), with lower velocity concentrations being observed closed to the bottom. However, in the case of a single gas injection, as the flow rate increasing the high-velocity region mainly concentrated at the corner of the measured flow domain. These observations suggest that the flow behavior under double and single gas injection is markedly different, and further investigation is warranted to better understand its underlying physical process.

A more detailed velocity magnitude analysis is presented in the Figs. 3 and 4, showing the mean volumetric velocity field in the x , y , and z directions for both double and single gas injections.

In the case of double gas injection, the volumetric flow field under the injection rate of 0.1 LPM exhibits a distinct behavior compared to the other conditions. The flow pattern of velocity in the x -direction shows high velocity concentration on diagonal corners that extend along the diagonal. For the y -direction velocity flow field, high velocity concentrations are observed at the center of the top boundary. Moving away from the center, a lower flow velocity surrounds the high velocity concentration, resulting in a concave bowl formation connected to the center line that extends downwards. For the z -direction velocity, the high velocity flow pattern is more concentrated at the center of the x -axis at the top boundary. As the injected gas flow rate increases, the flow pattern becomes more random, lacking a clear structure/pattern. In the case of a single gas injection, as the flow rate increases, the flow contour pattern remains consistent and becomes more distinct and prominent by intensifying the concentrated areas.

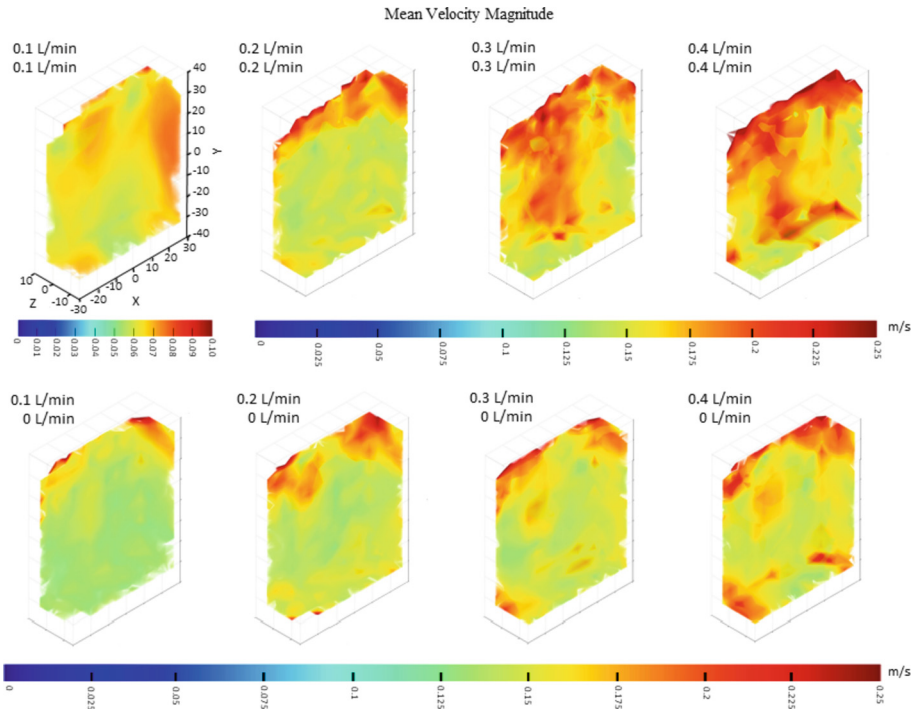


Fig. 2. Volumetric plot of the iso-surfaces of mean velocity magnitude.

3.2 Mean Velocity Streamlines

From the mean velocity field, the three-dimensional streamlines can be obtained and is a helpful tool for visualizing the fluid flow to understand the complex flow behavior. Figure 5 presents the three-dimensional streamlines for double and single gas injections. For double gas injection, at the lower flow rate of 0.1 L per minute, the three-dimensional streamlines are highly structured and organized. The flow follows a well-defined, well-organized pattern in X-Y planes with the streamlines being symmetrically distributed about the centerline in x direction. As the gas injection flow rate increasing, the streamlines become more complex and less organized. On the other hand, the streamline patterns for single gas injection are highly disordered and lack of clear pattern, even at low gas injection rates of 0.1 L per minutes. The streamlines do not follow any particular pattern, and there are groups or clusters in the flow region at any rate of gas injection.

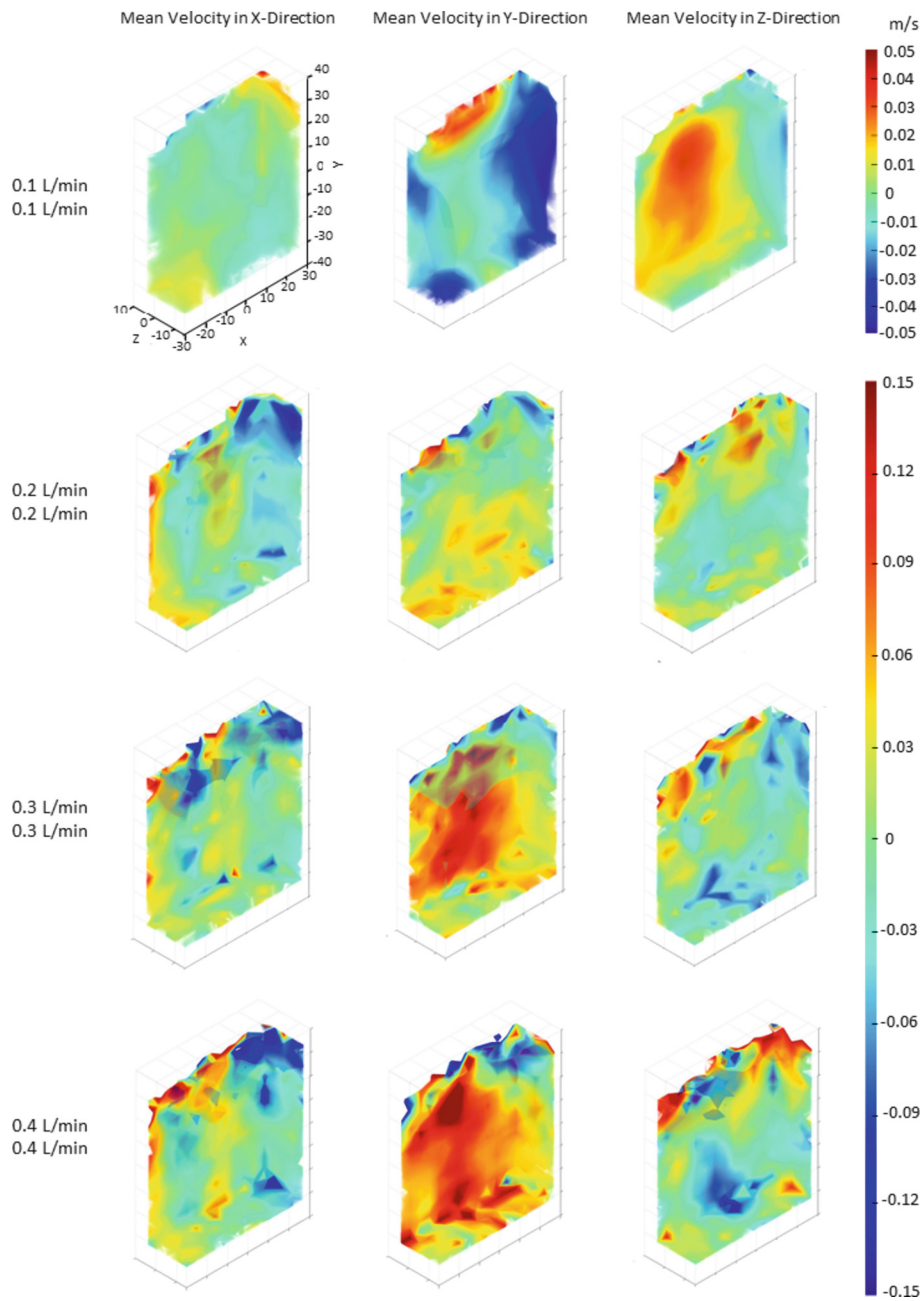


Fig. 3. Mean velocity field in X, Y, Z directions with double gas injections.

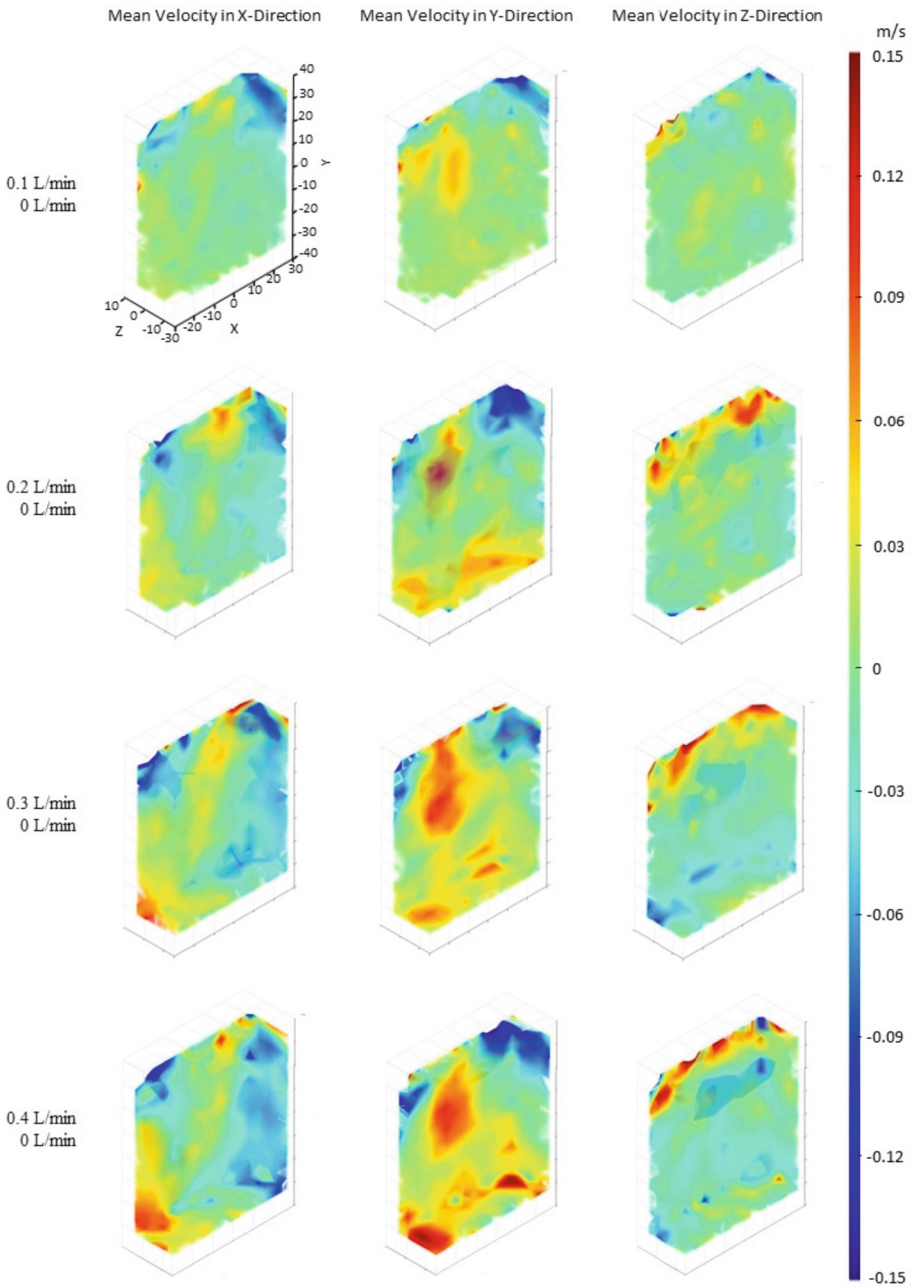


Fig. 4. Mean velocity field in X, Y, Z directions with single gas injection.

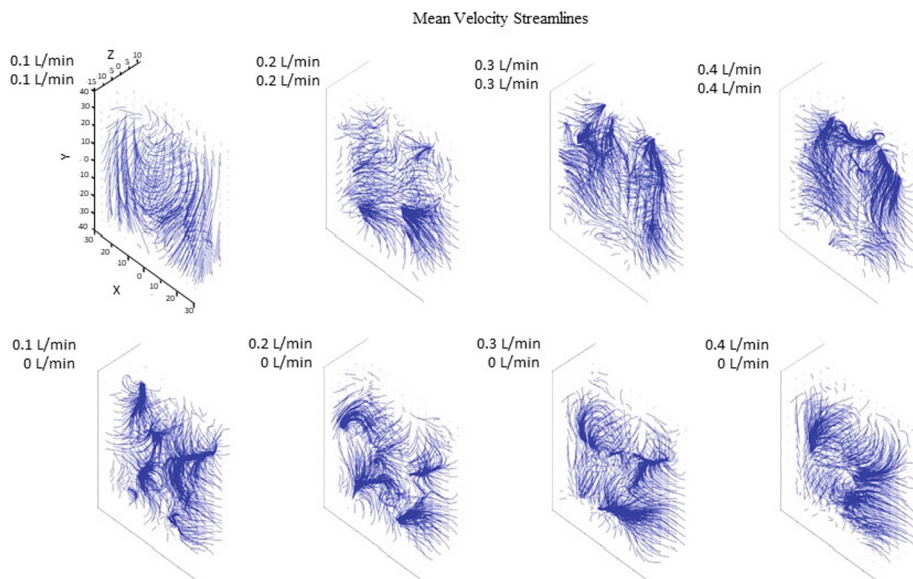


Fig. 5. 3D streamlines for mean velocity field.

When examining streamlines from mean velocity field on two dimensional planes, nodal points of separation and attachment, focus points of separation and attachment, and saddle points can be observed. A nodal point of attachment is a point in the flow field where the velocity lines are directed outward away from the node, while nodal points of separation are directed inward towards the node. On the other hand, a focus differs from a nodal point in that it spirals around the singular point, either from it (a focus of attachment) or into it (a focus of separation). At a saddle point, the streamlines are moving in different directions along two perpendicular planes, forming a point of flow stagnation. As the fluid moves away from the saddle point, it diverges in one direction and converges in the other direction, forming a region of flow separation. These findings are in line with previous studies that have shown the existence of these features in various fluid flow systems [15]. To illustrate these features, in Fig. 6 to Fig. 9, the streamline is plotted on the planes of the $x = -5$ mm, $y = -5$ mm and $z = -5$ mm with and without the velocity magnitude contour. The results showed that these characteristic points were presented in all planes and were clearly influenced by the gas injection flow rate. At lower gas injection flow rate, the streamlines tend to be more organized and follow a more predictable pattern, whereas at higher gas injection flow rate, the streamlines become more chaotic and disordered, making it difficult to discern any specific pattern or feature.

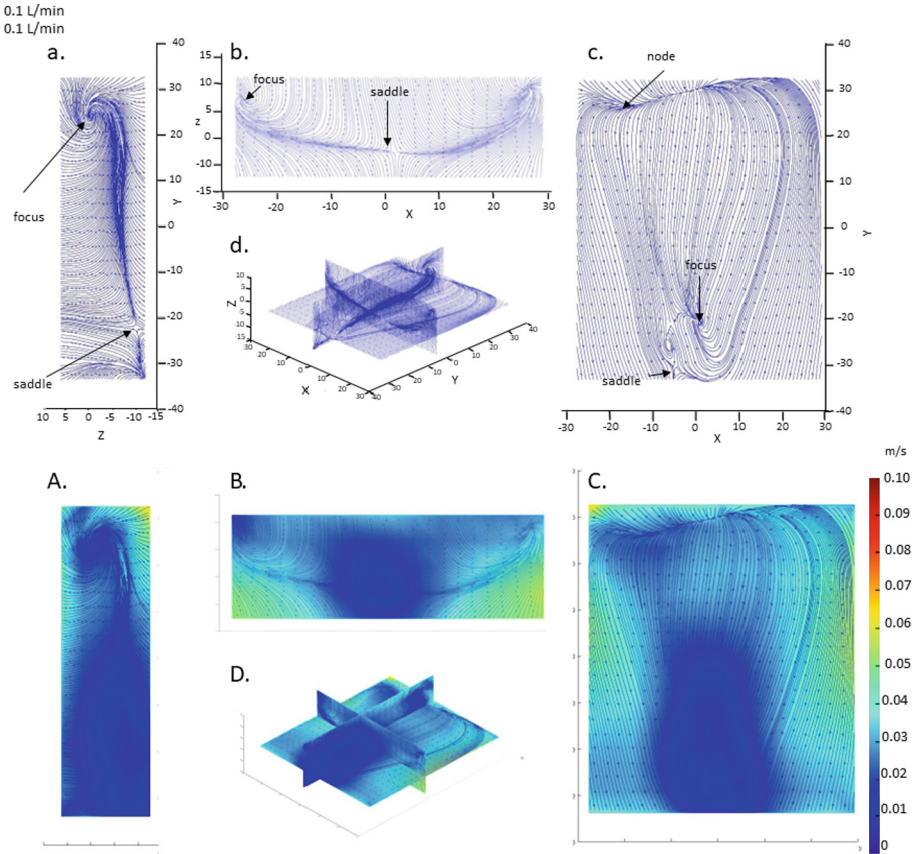


Fig. 6. Streamlines and velocity magnitude on different planes with double gas injection at 0.1 L/Min.

To further elaborate on the observation, Fig. 6 displays a clear and structured flow pattern for the double gas injection at a gas injection rate of 0.1 L per minute. In Fig. 6b, The X-Z plane at $z = -5$ mm exhibits a saddle point near the x-centerline where the flow move into opposite directions, leading to flow stagnation. The foci points are mirrored about this saddle point, which spirals around the singular point. In the X-Y plane (Fig. 6c), the streamlines illustrate an organized flow pattern with a slight deviation from perfect symmetry. Furthermore, downward flow momentum dominates the measured flow field opposing the direction of gas injection, and the low velocity is concentrated throughout the Z-Y plane (Fig. 6a, 6A), near the bottom boundary of the X-Y plane, and the center of X-Z plane (Fig. 6c and 6C). In Fig. 7, when the gas flow rate is increased to 0.3 LPM for the double gas injections, the flow starts to lack organized structure, like previously observed. Notably, the dominate momentum in the flow field changes from downward to upward. Additionally, high velocity is concentrated more throughout each plane and shows a more random pattern of flow compared to Fig. 6. Figure 8 presents the two-dimensional flow patter with single gas injection at a flow rate 0.1 L per minute. The

flow field lacks dominated momentum with certain direction and can be characterized by multiple directions present. Low velocity concentration dominates throughout the flow field, with high velocity on the tips of the top boundary, showing no clear pattern of the flow. Finally, Fig. 9 shows the results for a single gas injection at the highest gas injection rate of 0.4 L per minute. The flow is still disrupted and random with no dominated momentum. High velocity concentration is intensified at the outer boundaries with no clear/consistent pattern observed. Overall, 2D streamline visualization provides valuable insights into the fluid flow behavior and flow patterns. The results also suggest that the injection rate and the type of gas injection have a significant impact on the fluid flow behavior and the resulting streamline patterns. At lower flow rates, with double injections, the flow pattern is more structured and organized, whereas at higher flow rates, the flow becomes more random and chaotic. Additionally, the type of gas injection (single or double) can significantly affect the flow pattern.

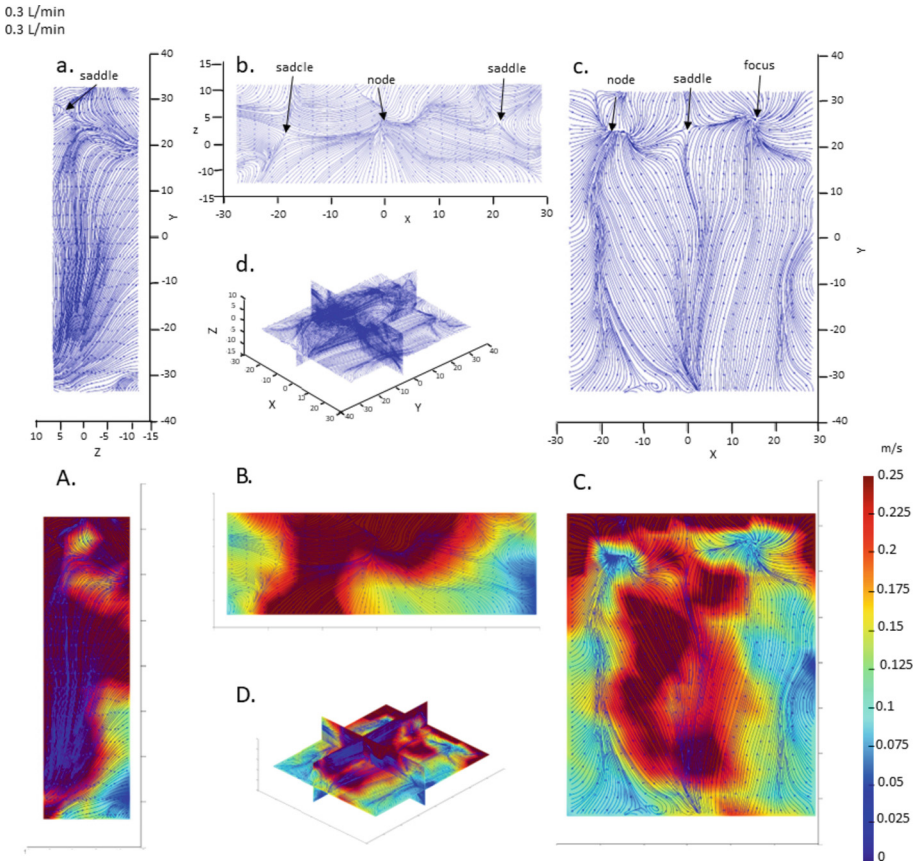


Fig. 7. Streamlines and velocity magnitude on different planes with double gas injection at 0.3 L/Min.

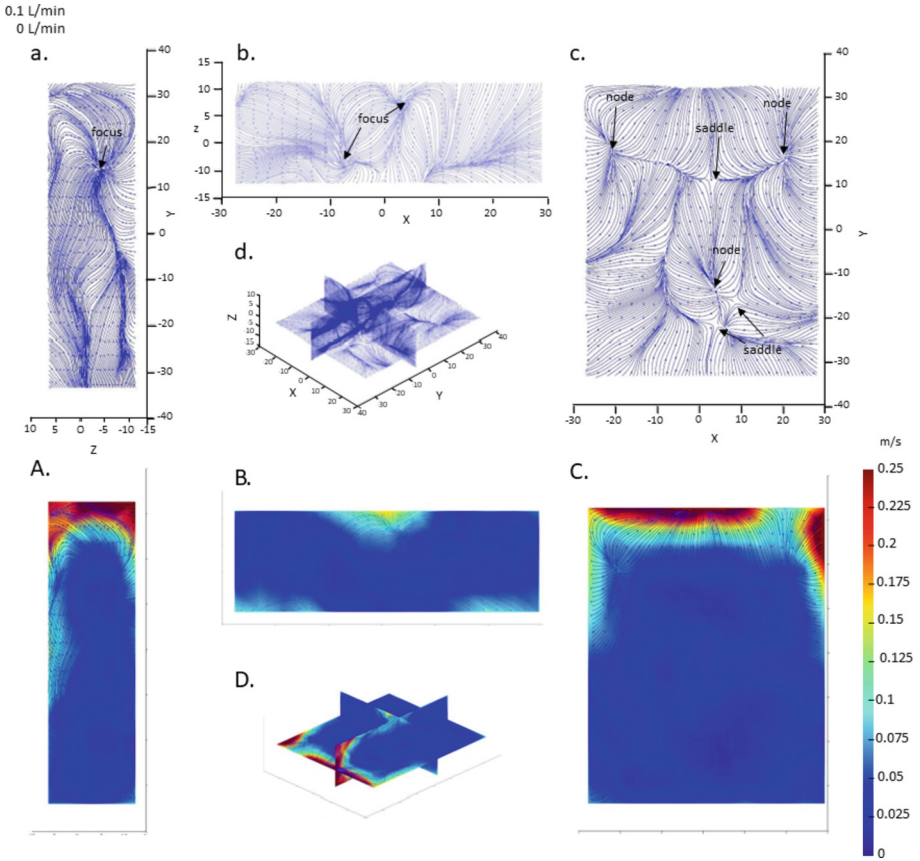


Fig. 8. Streamlines and velocity magnitude on different planes with single as injection at 0.1 L/Min.

4 Discussion

To gain a more comprehensive understanding of the complex process of ladle metallurgy, an analysis was conducted on the velocity distribution within the volumetric flow of a water ladle model, with results presented in Sect. 4.1. In Sect. 4.2, the findings of a Computational Fluid Dynamics (CFD) simulation of the same model are discussed and compared with the experimental data. Finally, a quantitative comparison between the experiment results and the CFD simulation is presented and reviewed.

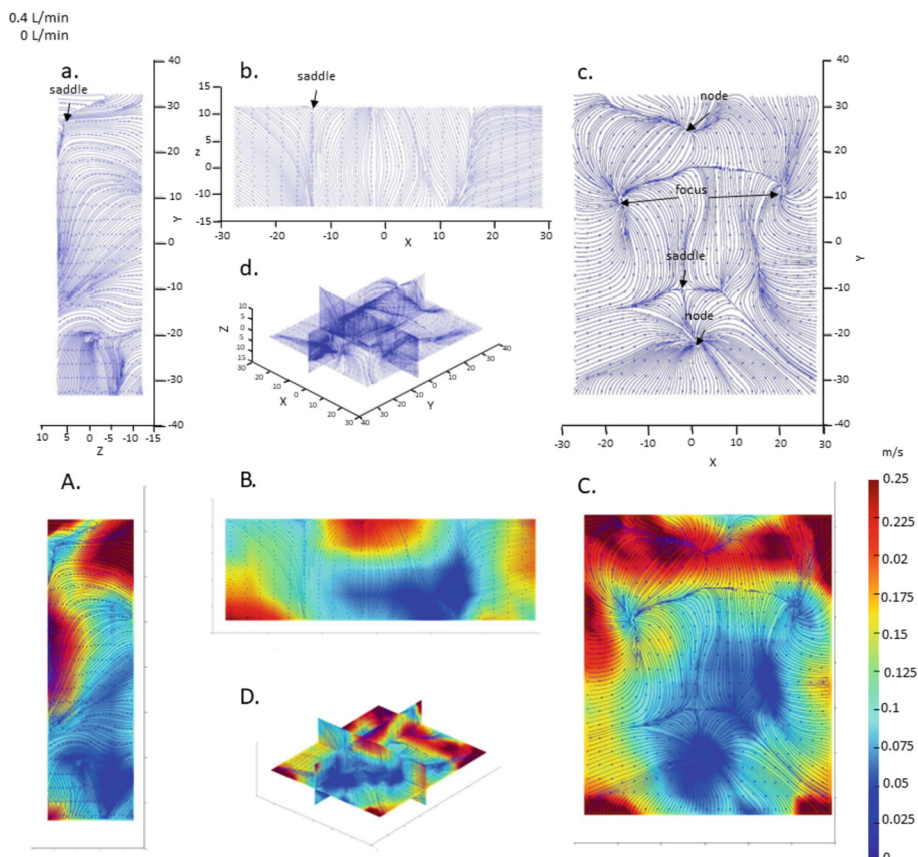


Fig. 9. Streamlines and velocity magnitude on different planes with single gas injection at 0.4 L/Min.

4.1 Transition of the flow pattern

Through the velocity field analysis in the volumetric flow inside the water ladle model using mean velocity magnitude (see Sect. 2.1) and streamlines (see Sect. 2.2), consistent trends have been revealed and can be validated across multiple figures. For double gas injection, as the gas flow rate increases, the high velocity concentration extended from top to bottom in the vertical direction, resulting in a more uniform flow with higher fluid velocity magnitude throughout the volumetric region as seen in Fig. 2 and Fig. 3. Further examination of the mean velocity field revealed a clear flow field transition with increased gas injections. With the flow rate of double gas injection increased from 0.1 to 0.2 L per minute, flow field changes from an organized and structured flow pattern to a disorderly, random, and unpredictable flow pattern, as seen in the mean velocity in the y -direction in Fig. 3. As the flow rate increases further, the disorderly flow pattern continues with elevated velocity magnitude throughout the studied region. The trend of increasing gas flow rates leading to irregular and asymmetrical flow patterns is also supported by a particularly clearer visual representation in Fig. 5, the mean 3D velocity

streamlines. With the gas injection flow rate increases from 0.1 to 0.2 L per minute, the symmetrical, organized and mostly vertical streamlines transition to an irregular and prominently horizontal streamlines. Not as pronounced but still visual, another transition occurs by increasing the flow rate again to 0.3 L per minute. This can be observed in the changes in the orientations of the streamlines, which become more vertical. Upon closer examination of the mean velocity streamlines at various planes with and without the mean velocity magnitude contour, further verification of the observed trends can be found in Fig. 6 and 7. Particularly, Fig. 6 confirms the highly organized, clear structure, and balanced flow pattern at a low double gas injection of flow rate at 0.1 L per minute. Additionally, it can be seen that downward momentum dominates the flow measurement region, despite the gas injection should introduce an upwards momentum. By investigating the streamlines and mean velocity on the stream-slices, it can be noted that low velocity concentrates around the focus point on the X-Y plane (Fig. 6c). The existence of focus point in the flow field is undesired and problematic as it causes fluid accumulation and prevents the refining process. As the gas flow rate is increased to 0.3 L per minute, in Fig. 7, the flow lacks an orderly structure. In this instance, the dominate flow direction of the flow field changes from downward to upward momentum with less outwards curvature. Additionally, high velocity is more concentrated throughout each plane. Therefore, these trends suggest that higher gas flow rates may be desirable to achieve the desired level of flow uniformity and to reduce the accumulation of stagnant fluid. For single gas injection, unlike double gas injection, increasing the gas flow rate did not lead to changes in the concentration contour or flow pattern. Instead, it enhanced the high velocity concentration and kept the contour pattern consistent, as demonstrated in Fig. 2 and Fig. 4. As the flow rate increases, the contour patterns of the high velocity regions become more pronounced and distinct. This suggests that the flow field is becoming more focused and concentrated as the gas flow rate increases, resulting in a higher concentration of fluid velocity in certain areas of the volume region. Additionally, as seen in Fig. 5, the streamlines continuously lack structure at any flow rate, exhibiting a chaotic, noisy, and irregular flow pattern with multiple directions and strong concentrated clusters. Further verification was obtained by examining the mean velocity streamlines at the planes of $x = -5$ mm, $y = -5$ mm, and $z = -5$ mm with and without the mean velocity magnitude contour, as shown in Fig. 8 and Fig. 9. Figure 8 confirmed the chaotic flow pattern and the absence of a dominant momentum direction, which could be the result of multiple nodal, focus, and saddle points. Moreover, the flow field was dominated by low velocity concentration, which could cause the fluid to be stationary less turbulent within the volume. With the flow rate increased to 0.4 L per minute, as demonstrated in Fig. 9, the flow remained disrupted with no dominate momentum. However, the concentration of high velocity was intensified and enhanced, extending to the outer boundaries and improving the fluid bulk motion. Overall, the analysis of single gas injection showed that increasing the gas injection flow rate can help the enhancement of high velocity concentration but did not significantly change the flow pattern or behavior.

By comparing the double and single gas injection, notable differences can be observed. In Fig. 2, the high velocity concentration of double injection is more evenly distributed on the top, whereas for a single injection, it concentrates on the edges of the top

boundary. As the flow rate increases, the high velocity concentration for single injection extends towards the middle of the top boundary, approaching that of double injection. At a flow rate of 0.1 L per minute, the flow was observed to be less organized. Figure 5 shows that double injections become more oriented in the upward/downward direction as the flow rate increases, while single injections continue to have fluid flow in multiple directions. Additionally, single injections have more concentrated groups, while double injections are more uniform throughout the region. In summary, the analysis of the data using various plots has revealed some common trends across different conditions. In the case of double injection at 0.1 LPM, the flow pattern exhibited irregularity phenomenon by having organized, symmetrical, and lowest velocity contour, with a dominant downward momentum in the flow. We suspect that this organized flow pattern is corresponded to the laminar flow. As the flow increased to 0.2 LPM and then 0.3 LPM, flow pattern transition is observed, possibly indicating a transition from laminar to turbulent flow. With the gas injection flow rate increases, high velocity concentration becomes more uniform throughout the flow field, extending from the top to the bottom of the flow field, and the momentum becomes more dominant in the upwards direction. On the other hand, for a single injection, the flow pattern was consistently disorderly and chaotic, with high concentration enhancing as the flow rate increased. This flow behavior is likely due to the unbalanced gas injection which leads to random and unpredictable fluid flow. The node, focus, and saddle points were also observed as the sources of velocity changes across all cases. These finding underscores the significance of careful consideration of injection method and flow rate for industrial applications aiming to achieve desired flow patterns.

4.2 Comparison with CFD Simulation

In recent years, CFD simulation has become the most commonly used method for studying complex fluid flow phenomena such as those encountered in industrial applications. However, due to the inherent complexities of the flow processes, there are still significant uncertainties associated with computational fluid dynamics (CFD) modeling. In order to address these uncertainties and validate the CFD simulation, experiment validation is highly desired. And experiments can provide valuable insights into the limitations and strengths of CFD modeling in capturing the complex flow behavior. In an ongoing research, a CFD simulation is conducted to simulate the complex flow field of the water ladle model that is implemented in the current volumetric flow measurement experiment. Preliminary results from the CFD experiment are shown in Fig. 10 where the simulated mean velocity field in x, y, and z directions with double gas injection at 0.1 L per minute is presented. The simulation has been performed using a VOF-DPM multiphase model to track multiphase interaction and interface behavior, and a Large Eddy Simulation (LES) turbulence model has been employed. In this setup, two injectors are placed at the bottom of the tank, each maintaining a constant flow rate of 0.1 LPM. A qualitative comparison of the velocity distribution in each component direction is presented in the figure. While the velocity distribution pattern is similar, the CFD results demonstrate a more symmetric behavior compared to the experimental results which might not be perfectly symmetric. Specifically, the velocity field in the x-direction has good compatibility while the velocity field in the y-direction is similar in the upper region with

higher velocity, but the CFD experiment shows a more intense velocity distribution with an over-predicted plume region. Therefore, these findings highlight the qualitative similarity of the flow field between the experiments and CFD simulations, suggesting the implemented numerical method can derive a reasonable and accurate flow field.

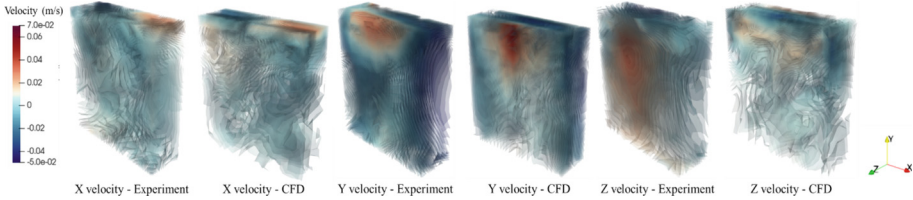


Fig. 10. CFD simulation of mean velocity field in X, Y, Z directions with double gas injections at 0.1 L/Min.

To achieve a quantitative comparison, the experimental and CFD flow field data are reprocessed to extract mean velocity plots that can be compared among the experiment and CFD results. Figure 11 presents the vertical velocity plots estimated on YZ planes and XY planes (mean value of vertical velocity is calculated on each planes along the X and Z directions) under double gas injection at 0.1 L per minute. Although the velocity distribution between the experimental data and the CFD simulation is similar, a noticeable discrepancy is observed. Specifically, the graph shows a vertical shift upward from the experimental data points. Despite this discrepancy, the overall trends match well between the experimental and simulated data, providing promising evidence for the validity of the CFD model. Further analysis is currently being conducted on the other conditions investigated in this project. The aim is to compare the CFD simulation results to the experimental data for all the compressed air injection conditions, to further validate the CFD model and assess its accuracy in predicting the flow behavior in the water ladle model.

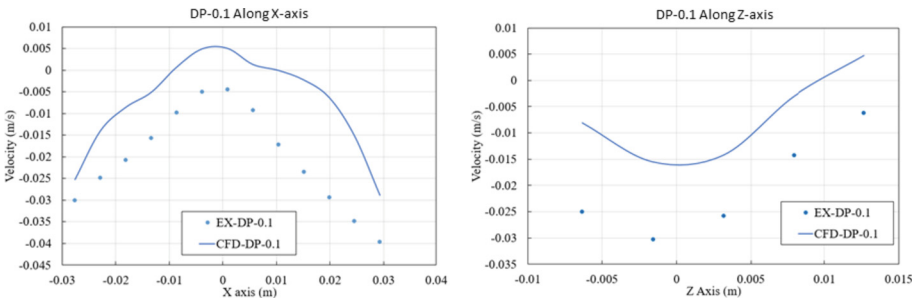


Fig. 11. Quantitative comparison of mean velocity field with double gas injections at 0.1 L/Min.

Acknowledgements. This work was supported in part by the National Science Foundation through its MRI program (CMMI-1919726) and GOALI program (CMMI-2113967). Support from all members of the Steel Manufacturing Simulation and Visualization Consortium (SMSVC), the SMSVC Ladle Project Technical Committee members, and Nucor Steel and the permission to publish this work are greatly acknowledged.

References

1. Mazumdar, D., Guthrie, R.I.L.: The physical and mathematical modelling of gas stirred ladle systems. *ISIJ Int.* **35**(1), 1–20 (1995)
2. Szekely, J., Asai, S.: The general mathematical statement of turbulent recirculatory flows. *Trans. Iron Steel Inst. Jpn.* **15**(5), 270–275 (1975)
3. DebRoy, T., Majumdar, A.K., Spalding, D.B.: *Appl. Math. Model.* **2**, 146 (1978)
4. Johansen, S.T., Robertson, D.G.C., Woje, K., Engh, T.: *Metall. Mater. Trans. B* **19**, 745 (1988)
5. Peranandhanthan, M., Mazumdar, D.: Modeling of slag eye area in argon stirred ladles. *ISIJ Int.* **50**(11), 1622–1631 (2010)
6. Mazumdar, D., Guthrie, R.I.L.: Modeling energy dissipation in slag-covered steel baths in steelmaking ladles. *Metall. Mater. Trans. B* **41**(5), 976–989 (2010)
7. Nunes, R.P., et al.: Visualisation and analysis of the fluid flow structure inside an elliptical steelmaking ladle through image processing techniques. *J. Eng. Sci. Technol.* **2**(2), 139–150 (2007)
8. Li, L., et al.: Water model and CFD-PBM coupled model of gas-liquid-slag three-phase flow in ladle metallurgy. *ISIJ Int.* **55**(7), 1337–1346 (2015)
9. Liu, Z., Li, L., Li, B.: Modeling of gas-steel-slag three-phase flow in ladle metallurgy: Part I. Physical modeling. *ISIJ Int.* **57**(11), 1971–1979 (2017)
10. Vazquez, A., et al.: A look at three measurement techniques for bubble size determination. *Exp. Thermal Fluid Sci.* **30**(1), 49–57 (2005)
11. Aoki, J., Thomas, B.G., Peter, J., Peaslee, K.D.: Experimental and theoretical investigation of mixing in a bottom gas-stirred ladle. In: *AISTech – Iron and Steel Technology Conference Proceedings*, vol. 1, pp. 1045–1056 (2004)
12. Fukuji, Y., Mori, Y., Fujita, S.: Sizes and size distributions of bubbles in a bubble column. *Chem. Eng. Jpn.* **12**(1), 5–9 (2006)
13. Owusu, K.B., et al.: Interaction of injector design, bubble size, flow structure, and turbulence in ladle metallurgy. *Steel Res. Int.* **90**(2), 1800346 (2019)
14. Schanz, D., Gesemann, S., Schröder, A.: Shake-the-box: Lagrangian particle tracking at high particle image densities. *Exp. Fluids* **57**(5) (2016). <https://doi.org/10.1007/s00348-016-2157-1>
15. Tobak, M., Peake, D.J.: Topology of three-dimensional separated flows. *Annu. Rev. Fluid Mech.* **14**(1), 61–85 (1982). <https://doi.org/10.1146/annurev.fl.14.010182.000425>